

NMR study of slow atomic motion in Sr₈Ga₁₆Ge₃₀ clathrate

Weiping Gou, Yang Li, Ji Chi, and Joseph H. Ross, Jr.

Department of Physics, Texas A&M University, College Station, Texas 77843-4242, USA

M. Beekman and G. S. Nolas

Department of Physics, University of South Florida, Tampa, Florida 33620-5700, USA

(Received 5 January 2005; revised manuscript received 2 March 2005; published 26 May 2005)

The clathrates feature large cages of silicon, germanium, or tin, with guest atoms in the cage centers. Sr₈Ga₁₆Ge₃₀ clathrate is interesting because of its thermoelectric efficiency, and its glasslike thermal conductivity at low temperatures, indicating Sr atom hopping within the cages. We measured ⁷¹Ga NMR with a 9 T superconducting spectrometer down to 1.9 K. Knight shift and T_1 results are consistent with low density metallic behavior. The lineshapes exhibit changes consistent with motional narrowing at low temperatures, and this indicates unusually slow hopping rates. Fitting these line shape changes yielded an activation energy of about 7 K. To further investigate this behavior, we made a series of measurements using the Carr-Purcell-Meiboom-Gill NMR sequence. Fitting the results to a hopping model yielded an activation energy of 4.6 K, consistent with the line shape result. We can understand all of our observations in terms of nonresonant atomic tunneling between asymmetric sites within the cages, in the presence of disorder.

DOI: 10.1103/PhysRevB.71.174307

PACS number(s): 63.20.Pw, 82.75.-z, 76.60.-k, 71.20.Nr

I. INTRODUCTION

Clathrates consist of cages of silicon, germanium, or tin in a crystalline framework, with guest atoms located inside the cages. Recently these materials have attracted considerable attention due to their thermal and thermoelectric properties. The type-I clathrates Sr₈Ga₁₆Ge₃₀ and Eu₈Ga₁₆Ge₃₀ have been observed to have glasslike thermal conductivity at low temperatures,¹ while Ba₈Ga₁₆Ge₃₀ does not behave this way. Structural studies performed on Sr₈Ga₁₆Ge₃₀, Ba₈Ga₁₆Ge₃₀, and Eu₈Ga₁₆Ge₃₀²⁻⁴ include single-crystal neutron-diffraction measurements, which showed that Sr and Eu atoms in the larger cages of the type-I structure have a small displacement off the center position to one of four crystallographically equivalent positions at low temperatures, while Ba atoms remain at the center. This provides a connection between the thermal response and atomic displacements within the cages. Recent low temperature ultrasonic attenuation measurements on a Sr₈Ga₁₆Ge₃₀ single crystal⁵ provided additional evidence for a relatively high concentration of tunneling states, a feature normally associated with bulk glasses like SiO₂.

In a recent paper on resonant ultrasound measurements,⁶ a specific model for the tunnel barriers between four-well tunneling states was described for the Eu clathrate. However the results for the Sr clathrate could be best fit by transitions between quantized Einstein modes of Sr atoms in the cages. The Einstein temperature is about 50 K in Sr clathrate.^{2,7,8} However the thermal conductivity observed at low temperatures indicates that disordered oscillator states with barrier heights smaller than the 50 K Einstein temperature must also be important.

The long coherence times allow nuclear magnetic resonance (NMR) to be used to study relatively low-frequency atomic dynamics. Thus, using ⁷¹Ga NMR, we can probe the low-temperature hopping of guest atoms in the cages. The magnetic moment of Eu produces large linewidths and fast

relaxation times, obscuring the hopping behavior in that case, however below we show that for the Sr clathrate, pulsed NMR techniques can resolve the relatively slow Sr hopping behavior at low temperatures. In addition, we describe Knight shift and T_1 relaxation results which provide a measure of the low-density conduction electron concentration in this material.

II. EXPERIMENTAL METHODS

Sr₈Ga₁₆Ge₃₀ crystals were prepared as follows.³ Stoichiometric quantities of the high-purity constituent elements were mixed and reacted in pyrolytic boron nitride (BN) crucibles for 24 h at 950 °C then annealed at 700 °C for 24 h. The BN crucibles were themselves sealed inside a fused quartz ampoule, which was evacuated and backfilled with nitrogen gas to a pressure of two-thirds of an atmosphere. The ingots were composed of crystallites with dimensions of one to three cubic millimeters. The ingots are stable in air and water but were etched with aqua regia for metallographic analysis, which indicated single-phase material. X-ray diffraction measurements were used for further characterization, which verified the crystallinity and phase purity of the specimen.

NMR experiments were performed at a fixed field of 9 T using a homebuilt pulse spectrometer.⁹ The field was calibrated using a Ga(NO₃)₃ dilute solution as ⁷¹Ga zero-shift reference (frequency close to 115 MHz). The sample for NMR measurements was several cubic millimeters, made into powder, and mixed with KBr.

III. MEASUREMENTS AND DISCUSSION

NMR spectra of Sr₈Ga₁₆Ge₃₀ at room temperature and 4.2 K are shown in Fig. 1, measured by echo integration. A room-temperature search over a considerably wider range of

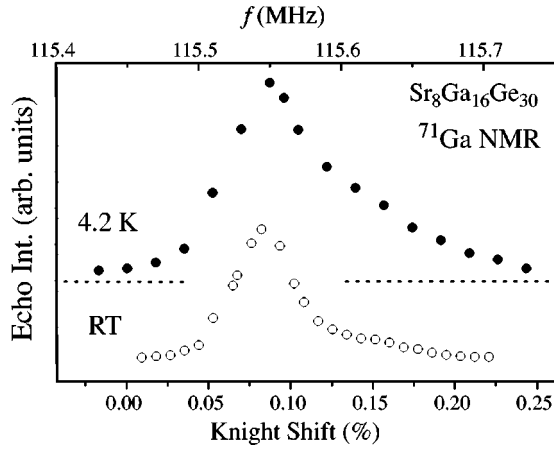


FIG. 1. Line shapes at room temperature and 4.2 K, offset vertically for clarity.

shifts verified this broadened line to be the only observable signal. Since it is known¹⁰ that Ga occupies all three crystallographic sites in $\text{Sr}_8\text{Ga}_{16}\text{Ge}_{30}$, the single NMR line observed at both temperatures is presumably due to a superposition of signals from these three sites, with their individual powder patterns.

Measured signals correspond to the central transition ($-1/2 \leftrightarrow 1/2$) for $I=3/2$ ^{71}Ga , which was confirmed by comparing the pulse length for the $\text{Ga}(\text{NO}_3)_3$ solution with those of the $\text{Sr}_8\text{Ga}_{16}\text{Ge}_{30}$ sample.¹¹ This situation is not uncommon in alloy samples, for which random quadrupole couplings can leave the satellite transitions broadened into a featureless background, with the relatively narrow central transition affected only to second order in the quadrupole coupling. T_1 measurements at the center of the line shape were done by use of the sequence $180_x-(T_{\text{wait}})-90_x-(\tau)-180_x-(\tau)$ -echo. The data were fitted to a multiexponential relaxation curve assuming magnetic relaxation for the central transition to obtain T_1 .¹² The data agreed well with these curves over the whole temperature range. The T_1 results are shown in Fig. 2. These data obey the Korringa relation, a signature of metallic behavior,¹³ with $T_1T=8.5$ sK obtained by least squares fitting. The Knight shift of the center of

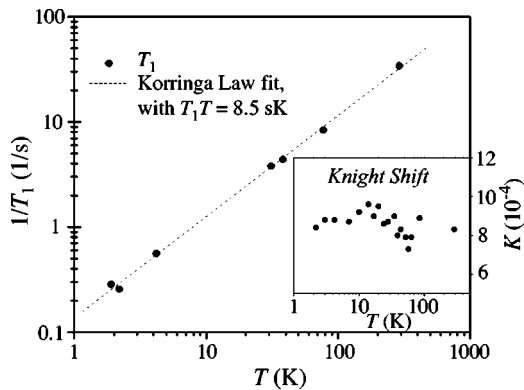


FIG. 2. Temperature dependence of ^{71}Ga T_1 ; experimental error bars are smaller than the symbol sizes. Dotted curve is a least squares fit to the Korringa Law. Inset: Knight shift of the center of mass, versus T .

mass of the line shape is almost independent of temperature around $K=0.084\%$ (Fig. 2 inset). These results indicate that T_1 and K are dominated by interactions with conduction electrons, and that $\text{Sr}_8\text{Ga}_{16}\text{Ge}_{30}$ is doped into the metallic regime. This is in agreement with electrical transport for this material,^{2,4,14} which typically indicates n -type behavior, and carrier densities in the range 10^{20} to 10^{21} cm^{-3} , due apparently to intrinsic defects.

Combining the observed T_1 and K to form the Korringa product yields $K^2T_1T=5.9 \times 10^{-6}$ sK. The free-electron value for ^{71}Ga is 2.73×10^{-6} sK, obtained from¹³

$$K^2T_1T = \frac{\hbar}{4\pi k} \frac{\gamma_e^2}{\gamma_n^2}, \quad (1)$$

where γ_e is the gyromagnetic ratio of the electron, γ_n is the gyromagnetic ratio of the nucleus, and k is the Boltzmann constant. The observed Korringa product is enhanced by a factor of approximately 2.2, which is typical of ordinary metals, and indicative of normal metallic behavior. By contrast the Korringa product in disordered systems containing localized electrons will be strongly enhanced,^{15,16} a signature of the effects of the strong correlations.^{17,18} Note that in $\text{Na}_x\text{Ba}_y\text{Si}_{46}$ clathrate, a similar modest Korringa enhancement has been observed.¹⁹ However, in that case, K is temperature dependent, indicating possible sharp features in the electronic structure,²⁰ for which there is no evidence in the present case.

For further analysis, we used a parabolic band approximation to estimate K . We assume a spherical Fermi surface, with a conduction band s -orbital fraction equal to $1/4$ (corresponding to sp^3 hybridization) $m^*=3m_e$ and $n=1.5 \times 10^{20}$ cm^{-3} , which are typical values for samples of this material,¹⁴ and the hyperfine field for Ga, $H_{\text{HF}}=620$ T.²¹ These values yield $K=0.2\%$, which is slightly larger than observed. Thus, the relatively small K is consistent with the accepted electrical properties of $\text{Sr}_8\text{Ga}_{16}\text{Ge}_{30}$. Note that the quantity which we identify as K is actually an average of individual K values from among the three crystallographically inequivalent framework sites, because of the overlapping of lines. NMR lines for these sites can be seen individually in ^{29}Si NMR (Ref. 19) or possibly partially separated by magic angle spinning in Ga NMR.²²

The second-order quadrupole coupling can give further line shifts for the central transition, as well as broadening the line. To analyze for this effect, we performed ^{69}Ga NMR measurements at room temperature. We found that the center shift is 0.085% for ^{69}Ga , compared to 0.084% for ^{71}Ga . ^{69}Ga has a quadrupole moment $Q=0.178 \times 10^{-28}$ m^2 , compared to 0.112×10^{-28} m^2 for ^{71}Ga , and the second-order quadrupole shift is proportional to Q^2 .¹³ The small observed difference is comparable to the experimental error, and indicates that the second-order quadrupole contribution to this shift is very small. This justifies the approximation used above, in which the center shift was interpreted as a Knight shift, of magnetic origin. Furthermore, we found that the linewidth for ^{69}Ga exceeds that of ^{71}Ga , with a ratio of the full widths at half maximum equal to 2.34, which is slightly smaller than the ratio, $(Q^{(69)}/Q^{(71)})^2=2.53$, expected for broadening due en-

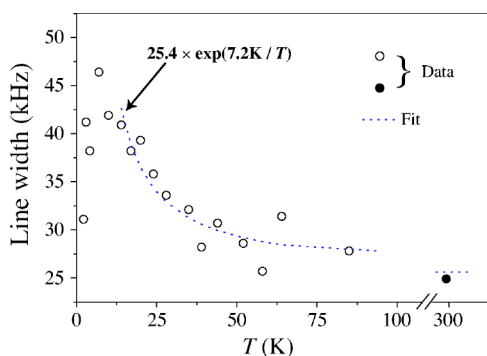


FIG. 3. ^{71}Ga NMR linewidth (square root of second moment) versus temperature, with activated fit described in text.

tirely to the second-order quadrupole coupling. This indicates that the broadening can be attributed mostly to quadrupole coupling, with a small additional anisotropic or inhomogeneous magnetic contribution.

The temperature dependence of the ^{71}Ga linewidth, obtained by calculating the square root of the second moment of the measured line, is shown in Fig. 3. The measured data for this calculation were obtained by fast Fourier transform (FFT) of the spin echo, which was obtained using shortened pulses to enhance the observation range. There is a significant increase in the linewidth at low temperatures (above 4 K). This change is apparently not due to an electronic structure change since K and K^2T_1T do not change. Instead, this change can be attributed to atomic motion. For this mechanism, assuming that the reduced high-temperature width is due to motional narrowing, the relevant time scale can be estimated by $1/\text{linewidth}$, roughly 10^{-5} s, since this is the time scale for narrowing of an NMR line. This is very slow compared to thermal vibration rates, for example 10^{12} Hz for the Einstein mode of guest atoms in the relatively open type-I clathrate cages.²

For random hopping, the linewidth can be related to a correlation time, which will follow $\tau_c = \tau_\infty \exp(E_a/kT)$ in the case of an activated process, where E_a is the activation energy of the system. Motions of atoms in the near vicinity of the Ga nuclei being observed will cause changes in the electric field gradient, and thus shifts in the NMR resonance position, due to the electric quadrupole effect. Because of the superposition of many orientations, we can see only a broadening, rather than a splitting or shift. In the motionally narrowed limit, the excess linewidth is proportional to τ_c , so that the linewidth can be fitted to $W_c = W_\infty \exp(E_a/kT)$ to find E_a . Fitting this expression to the high- T tail we find that E_a is 7.2 K. This fitted curve is shown in Fig. 3.

As a further measure of the dynamics, the spin-echo decay was measured by use of the standard Hahn spin echo sequence. The results are shown by Fig. 4. The data were fitted by

$$S = A\{\alpha \exp(-t/T_{2e}) + \exp[-(t/T_{2g})^2]\}. \quad (2)$$

Generally, an exponential decay is observed where motion is important, while Gaussian decay is characteristic of the static NMR line, dominated by the nuclear dipole-dipole or

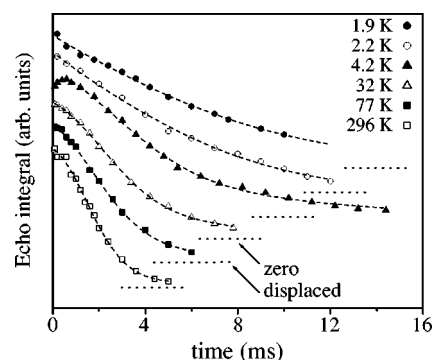


FIG. 4. Spin echo decay rate at different temperatures, with fits described in text

pseudodipolar couplings.²³ Thus the ratio α is a measure of the relative importance of motion.

The fitting results are shown in Table I. At low T , α is large, and the decay curve is exponential, which indicates that the echo decay is dominated by motion. However at high T , α is small, indicating that the motional contribution is averaged out, leaving a Gaussian decay due to like-spin coupling.²³ At high T , fast motion will cause more of the spin-spin coupling to be like-spin in character, which makes T_{2g} shorter. This is consistent with the observed behavior, and thus the picture established above, whereby the NMR line is subject to progressive motional narrowing as the temperature is raised, agrees with the spin-echo decay results.

In order to further understand the motion process, we performed measurements using the Carr-Purcell-Meiboom-Gill (CPMG) pulse sequence. The sequence is $90_x-(\tau)-[180_y-(\tau)\text{-echo}-(\tau)]^n$, where τ is half of the spacing between 180° pulses. The results at RT, 77 K, 32 K, and 4.2 K are shown by Fig. 5. We can see that as τ decreases, the echo decay rate becomes smaller, at all temperatures. One common mechanism for this type of decay in a CPMG experiment is diffusion of the atoms under observation. However, since the Ga atoms are bonded to the framework, low-temperature Ga motion seems very unlikely, and indeed we find that the $\exp(-t^3)$ behavior expected in this case¹³ does not fit the data very well. Sr-atom motions, however, can slowly modulate the Ga-site quadrupole shifts, providing a decay similar to what we observed. We cannot tell solely from these results whether Sr atoms are hopping between cages or between sites within the same cage, however since the energy barrier is evidently quite small, we will assume that these dynamics are associated with the rattling-type motion of Sr within the

TABLE I. Fitting result of the spin echo measurements.

Temperature (K)	T_{2e} (ms)	T_{2g} (ms)	α
1.9	8.1 ± 1.5	7.7 ± 3.6	5.0 ± 2.8
2.2	5.6 ± 0.1	7.7 ± 0.1	2.5 ± 0.1
4.2	6.7 ± 0.6	4.6 ± 0.2	1.3 ± 0.4
32	5.2 ± 0.5	3.3 ± 0.1	0.8 ± 0.2
77	3.4 ± 0.4	2.9 ± 0.3	0.8 ± 0.2
296	2.3 ± 0.6	2.2 ± 0.1	0.3 ± 0.1

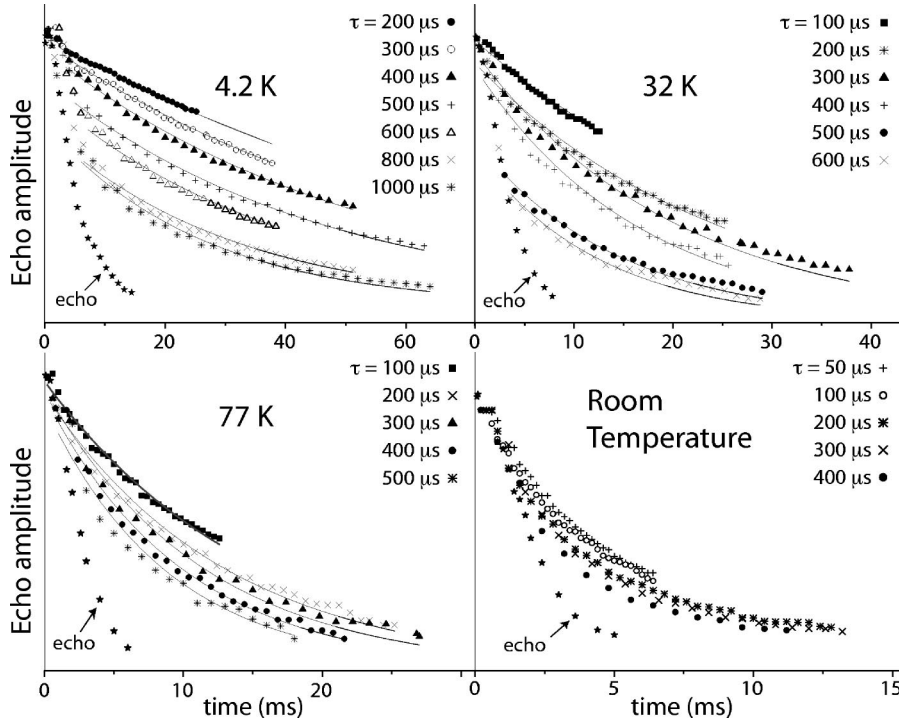


FIG. 5. CPMG measurements at different temperatures. Solid curves for 4.2, 32, and 77 K are fits described in text.

large cage, as has been discussed previously.²⁻⁴

To interpret the data, we have invoked a simplified model in which Sr atoms jump randomly between two positions, making nearby Ga nuclei change resonant frequencies by a difference $\Delta\nu$. $\Delta\nu$ will have a range of values according to Ga position and crystal orientation. During the calculation we made several assumptions: (1) the motion is very slow, so that normally only one jump occurs between 180° pulses; (2) $\Delta\nu$ has an exponential distribution of the form $P(\Delta\nu) = \exp(-\Delta\nu/\nu_1)/\nu_1$; and (3) $4\pi\tau_c\nu_1 \gg 1$, where τ_c is the correlation time. Based on these assumptions, we find that the spin echo amplitude can be expressed as

$$S = A \exp\left(\frac{-t}{T_2}\right) \exp\left(\frac{-t}{\tau_c}\right) \left[1 + \frac{\arctan(2\pi\nu_1\tau)}{\pi\tau_c\nu_1} \right]^{t/2\tau}, \quad (3)$$

where T_2 is the spin-spin relaxation time. In the CPMG experiments, the motion-free decay rate [$1/T_2$ in Eq. (3)] in fact differs from the normal spin-spin T_2 , since spin locking leads to a lengthened decay time close to T_1 [it is essentially $T_{1\rho}$ (Ref. 13)]. Spin-locking can be eliminated by the use of a phase-alternating pulse sequence (PAPS),²⁴ however measurements using a PAPS in our case yielded ill-formed echoes, due to the superposition of stimulated echoes.²⁵ Stimulated echoes can be minimized by a perfectly set 180° pulse, however the large linewidth makes this difficult in the

TABLE II. Fitting result of CPMG measurements.

Temperature (K)	T_2 (ms)	τ_c (ms)	ν_1 (kHz)
4.2	100	9.2	0.15
32	44	3.6	0.15
77	18	3.2	0.15

present case. Therefore, we used the standard CPMG sequence, making the spin-locking T_2 an adjustable variable.

We found that RT data did not fit Eq. (3) very well, presumably because the high-temperature T_1 is too short to develop complete spin locking. Therefore we fit the data for the other three temperatures to Eq. (3). The fitting results are shown in Table II. The results show that the typical Ga Larmor frequency difference ν_1 , which may vary due to the Ga atom's distance from and orientation relative to the moving Sr, is 0.15 kHz. We also fitted the resulting correlation times to the activation energy formula $\tau_c = \tau_\infty \exp(E_a/kT)$. Figure 6 is the result for this fit, which yields an activation energy $E_a = 4.6$ K. This value is close to the E_a obtained from line-width measurements.

We have made NMR measurements on several samples of $\text{Ba}_8\text{Ga}_{16}\text{Ge}_{30}$, which is the structural analog of $\text{Sr}_8\text{Ga}_{16}\text{Ge}_{30}$, however we find that variability of the Ba clathrate electronic properties obscures the effect being examined in this paper. $\text{Ba}_8\text{Ga}_{16}\text{Ge}_{30}$ is electrically very similar to $\text{Sr}_8\text{Ga}_{16}\text{Ge}_{30}$, but diffraction measurements indicate that the Ba atoms remain

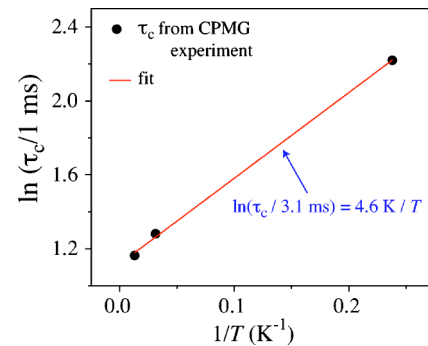


FIG. 6. Correlation time versus temperature. (Solid line is the fitting result according to activation energy formula.)

at the cage centers, in contrast to the Sr behavior. (Note, however, that a recent report²⁶ indicates that *p*-type Ba clathrate may share the amorphouslike thermal conductivity.) For all samples we have studied, Ga NMR in $\text{Ba}_8\text{Ga}_{16}\text{Ge}_{30}$ exhibits a larger linewidth than in $\text{Sr}_8\text{Ga}_{16}\text{Ge}_{30}$, and the T_1 deviates from a Korringa relation at low temperatures, in contrast to the simple-metallic behavior seen in $\text{Sr}_8\text{Ga}_{16}\text{Ge}_{30}$. There is also a small temperature dependence to the center shift of the Ba-clathrate resonance, not seen in the Sr clathrate. These results are consistent with a tendency toward carrier freezeout in the Ba clathrate, and the development of a dilute set of magnetic moments due to these localized carriers, or possibly the presence of narrow features in the electronic density of states, such as exhibited in $\text{Na}_x\text{Ba}_y\text{Si}_{46}$ clathrate.²⁰ This behavior unfortunately has precluded the comparison of Sr motion to the corresponding behavior in the Ba clathrate. We are continuing our studies of the electronic properties of the Ba clathrate and will report more detail at a later date.

Zerec *et al.*⁶ have examined a model of azimuthal four-well tunneling for the Eu clathrate, and their experimental resonant ultrasonic data could be fit satisfactorily by considering a four level tunnel system with well-defined barriers that are the same for each cage. However for Sr clathrate, the model did not work well, and the best fit was obtained assuming that the transitions took place between energy levels of the overall harmonic potential well for the Sr atom in its cage. This corresponds to a very large energy difference. In our experiment we find a small energy barrier with value close to 5 K. This is consistent with the thermal conductivity experiments¹ observed at temperatures below 1 K, and confirms that transitions between small energy levels play an important role. It is unclear whether this picture also provides a good fit to the resonant ultrasound measurements,⁶ however clearly there must be higher-energy excitations corresponding to the observed Einstein mode,^{2,7,8} in addition to the lower-frequency fluctuations which have a more prominent effect on the NMR measurements. Thus it seems possible that a model which combines these pictures may be consistent with the resonant ultrasound as well as the NMR results.

A Fourier map obtained from neutron-diffraction measurements showed that each Sr atom has a displacement roughly 0.3 Å from the center of the cage at low T .⁵ In order to approximate the tunneling rates, we first consider a simplified two level system consisting of an infinite square well modified to have a square barrier at its center. For an infinite square well having width 0.6 Å plus a barrier having width 0.2 Å and height 60 K, there are eigenstates with energy 32.2 and 38.1 K, giving a tunnel splitting of 5.9 K. This is similar to the activation barrier we observed, however the corresponding tunneling frequency is 10^{11} Hz (the splitting expressed in frequency units). This certainly cannot correspond to the situation in the Sr clathrate, for which the dynamics include slow motions of the order 10^5 Hz, as evidenced by the NMR. Thus we conclude that the activation energy observed by NMR cannot be a tunnel splitting between symmetric well states.

An asymmetric well can dramatically reduce the tunnel rate,^{27,28} and also can explain the linewidth increase with

temperature decrease because of different Ga Larmor frequencies for Sr at different sites.¹³ Considering a general situation of an asymmetric double well potential with two low-lying states differing by energy Δ , and a potential barrier between them with a tunneling rate Δ_0/\hbar , it can be shown²⁹ that the energy splitting between the two eigenstates is

$$\Delta E = \sqrt{\Delta^2 + \Delta_0^2}. \quad (4)$$

This is the model often used for two level systems (TLS) in glassy materials. For a symmetric TLS, where $\Delta=0$, the energy splitting of the two states will be the exact tunneling energy. In our systems, we observed a barrier of roughly 5 K, in which case the corresponding tunneling frequency will be 10^{11} Hz. Again this is not what we observed in our experiments. However for an asymmetric TLS, where $\Delta \neq 0$, from the above expression, Δ_0 can be much smaller than ΔE , so the tunneling rate can be dramatically reduced. A broad range of asymmetry parameters is found in many glassy systems, and this is the common way to understand the T^2 behavior of the thermal conductivity.

Thus, we can understand our observations in terms of nonresonant atomic tunneling between asymmetric sites within the cages, in the presence of disorder. There are various possibilities for the source of this disorder. For example, it is known that the Ga atoms are distributed on these framework sites.¹⁰ Furthermore, Sr vacancies or cage-cage interaction might also contribute. It is true that neutron diffraction measurements show four equivalent positions for each Sr atom,⁵ however this is not inconsistent with an asymmetric well, as long as the asymmetry is randomly distributed, since the scattering experiments do not distinguish static from transient disorder.

One thing that this model cannot explain is the linewidth decrease at the lowest temperatures (below 4 K, see Fig. 3). One possible explanation could be that at very low temperatures the displacement of the guest atoms assumes an ordered configuration. A similar result has been found for Si clathrates,³⁰ in which cage-centered sodium atoms are observed to dimerize at low temperatures. A configuration of this type could result in a decreasing linewidth due to decreased strain in the lattice.

IV. CONCLUSIONS

In Ga NMR measurements, we observed linewidth changes indicating slow atomic motion in the Sr clathrate. CPMG measurements yielded results that are consistent with the linewidth changes, assuming the mechanism to be hopping of Sr atoms within the cages. By a simple model, we obtained an activation energy $E_a=4.6$ K for Sr hopping, which is similar to the value obtained from linewidth measurements. This model assumed a wide distribution of hopping rates, and an asymmetric well model worked well to explain the data. The T_1 of $\text{Sr}_8\text{Ga}_{16}\text{Ge}_{30}$ obeys a Korringa relation, implying normal metallic behavior for the Sr clathrate, as expected for a heavily doped *n*-type semiconductor.

ACKNOWLEDGMENTS

This work was supported by the Robert A. Welch Foundation, Grant No. A-1526, by the National Science Founda-

tion (DMR-0103455), and by Texas A&M University through the Telecommunications and Informatics Task Force. M.B. acknowledges support from the University of South Florida.

-
- ¹J. L. Cohn, G. S. Nolas, V. Fessatidis, T. H. Metcalf, and G. A. Slack, *Phys. Rev. Lett.* **82**, 779 (1999).
- ²B. C. Sales, B. C. Chakoumakos, R. Jin, J. R. Thompson, and D. Mandrus, *Phys. Rev. B* **63**, 245113 (2001).
- ³G. S. Nolas, T. J. R. Weakley, J. L. Cohn, and R. Sharma, *Phys. Rev. B* **61**, 3845 (2000).
- ⁴L. Qiu, I. P. Swainson, G. S. Nolas, and M. A. White, *Phys. Rev. B* **70**, 035208 (2004).
- ⁵V. Keppens, B. C. Sales, D. Mandrus, B. C. Chakoumakos, and C. Laermants, *Philos. Mag. Lett.* **80**, 807 (2000).
- ⁶I. Zerec, V. Keppens, M. A. McGuire, D. Mandrus, B. C. Sales, and P. Thalmeier, *Phys. Rev. Lett.* **92**, 185502 (2004).
- ⁷G. S. Nolas and C. A. Kendziora, *Phys. Rev. B* **62**, 7157 (2000).
- ⁸B. C. Chakoumakos, B. C. Sales, D. G. Mandrus, and G. S. Nolas, *J. Alloys Compd.* **296**, 80 (2000).
- ⁹C.-S. Lue and J. H. Ross, Jr., *Phys. Rev. B* **58**, 9763 (1998).
- ¹⁰Y. Zhang, P. L. Lee, G. S. Nolas, and A. P. Wilkinson, *Appl. Phys. Lett.* **80**, 2931 (2002).
- ¹¹O. Kanert and M. Mehring, in *NMR: Basic Principles and Progress*, edited by E. Fluck and R. Kosfeld (Springer-Verlag, New York, 1971), Vol. 3, p. 1.
- ¹²A. Narath, *Phys. Rev.* **162**, 320 (1967).
- ¹³C. P. Slichter, *Principles of Magnetic Resonance* (Springer-Verlag, New York, 1989).
- ¹⁴V. L. Kuznetsov, L. A. Kuznetsova, A. E. Kaliazin, and D. M. Rowe, *J. Appl. Phys.* **11**, 7871 (2000).
- ¹⁵H. Alloul and P. Dellouve, *Phys. Rev. Lett.* **59**, 578 (1987).
- ¹⁶B. S. Shastry and E. Abrahams, *Phys. Rev. Lett.* **72**, 1933 (1994).
- ¹⁷D. Pines, *Phys. Rev.* **92**, 626 (1953).
- ¹⁸T. Moriya, *J. Phys. Soc. Jpn.* **18**, 516 (1963).
- ¹⁹F. Shimizu, Y. Maniwa, K. Kume, H. Kawaji, S. Yamanaka, and M. Ishikawa, *Phys. Rev. B* **54**, 13242 (1996).
- ²⁰J. Gryko, P. F. McMillan, R. F. Marzke, A. P. Dodokin, A. A. Demkov, and O. F. Sankey, *Phys. Rev. B* **57**, 4172 (1998).
- ²¹G. C. Carter, L. H. Bennett, and D. J. Kahan, *Metallic Shifts in NMR* (Pergamon, New York, 1977).
- ²²S. E. Lattner, J. D. Bryan, N. Blake, H. Metiu, and G. D. Stucky, *Inorg. Chem.* **41**, 3956 (2002).
- ²³A. Abragam, *Principles of Nuclear Magnetism* (Oxford University New York, 1983).
- ²⁴B. J. Suh, F. Borsa, and D. R. Torgeson, *J. Magn. Reson., Ser. A* **110**, 58 (1994).
- ²⁵R. L. Vold, R. R. Vold, and H. E. Simon, *J. Magn. Reson.* (1969-1992) **11**, 283 (1973).
- ²⁶A. Bentien, M. Christensen, J. D. Bryan, A. Sanchez, S. Paschen, F. Steglich, G. D. Stucky, and B. B. Iversen, *Phys. Rev. B* **69**, 045107 (2004).
- ²⁷D. L. Cox and A. Zawadowski, *Adv. Phys.* **47**, 599 (1998).
- ²⁸P. Esquinazi, *Tunneling Systems in Amorphous and Crystalline Solids* (Springer-Verlag, New York, 1998).
- ²⁹A. Halbritter, L. Borda, and A. Zawadowski, *Adv. Phys.* **53**, 939 (2004).
- ³⁰F. Tournus, B. Masenelli, P. Mélinon, D. Connétable, X. Blase, A. M. Flank, P. Lagarde, C. Cros, and M. Pouchard, *Phys. Rev. B* **69**, 035208 (2004).